Neuro-Oncology

Neuro-Oncology 18(7), 950–961, 2016
doi:10.1093/neuonc/nov315
Advance Access date 10 January 2016

An intrinsic DFF40/CAD endonuclease deficiency impairs oligonucleosomal DNA hydrolysis during caspase-dependent cell death: a common trait in human glioblastoma cells

María Sánchez-Osuna, Laura Martínez-Escardó, Carla Granados-Colomina, Fina Martínez-Soler, Sònia Pascual-Guiral, Victoria Iglesias-Guimarais, Roser Velasco, Gerard Plans, Noemi Vidal, Avelina Tortosa, Carlos Barcia, Jordi Bruna†, and Victor J. Yuste

Cell Death, Senescence and Survival group, Department of Biochemistry and Molecular Biology and Institute of Neurosciences, Faculty of Medicine, Universitat Autònoma de Barcelona, Barcelona, Spain (M.S.-O., L.M.-E., C.G.-C., S.P.-G., V.I.-G., V.J.Y.); Centro de Investigación Biomédica en Red sobre Enfermedades Neurodegenerativas (C.I.B.E.R.N.E.D.), Barcelona, Spain (M.S.-O., V.I.-G., V.J.Y.); Department of Basic Nursing, Institut d'Investigació Biomèdica de Bellvitge-Universitat de Barcelona, Barcelona, Spain (F.M.-S., A.T.); Unit of Neuro-Oncology, Hospital Universitari de Bellvitge-I.C.O Duran i Reynals, Barcelona, Spain (R.V., G.P., N.V., J.B.); Group of Neuroplasticity and Regeneration (C.I.B.E.R.N.E.D.), Department of Cell Biology, Physiology and Immunology & Institute of Neurosciences, Universitat Autònoma de Barcelona, Barcelona, Spain (R.V., J.B.); Neuropathology Institute, Hospital Universitari de Bellvitge, Barcelona, Spain (N.V.); Neuro-Immunity Group, Department of Biochemistry and Molecular Biology and Institute of Neurosciences, Faculty of Medicine, Universitat Autònoma de Barcelona, Barcelona, Spain (C.B.)

Corresponding Author: Victor J. Yuste, MD, PhD, Departament de Bioquímica i Biologia Molecular, Facultat de Medicina, Universitat Autònoma de Barcelona, Campus de Bellaterra, 08193 Bellaterra, Barcelona, Spain (victor.yuste@uab.cat).

†Jordi Bruna and Victor J. Yuste should be considered as co-senior authors.

Background. Glioblastoma (GBM) or grade IV astrocytoma is one of the most devastating human cancers. The loss of DFF40/CAD, the key endonuclease that triggers oligonucleosomal DNA fragmentation during apoptosis, has been linked to genomic instability and cell survival after radiation. Despite the near inevitability of GBM tumor recurrence after treatment, the relationship between DFF40/CAD and GBM remains unexplored.

Methods. We studied the apoptotic behavior of human GBM-derived cells after apoptotic insult. We analyzed caspase activation and the protein levels and subcellular localization of DFF40/CAD apoptotic endonuclease. DFF40/CAD was also evaluated in histological sections from astrocytic tumors and nontumoral human brain.

Results. We showed that GBM cells undergo incomplete apoptosis without generating oligonucleosomal DNA degradation despite the correct activation of executioner caspases. The major defect of GBM cells relied on the improper accumulation of DFF40/CAD at the nucleoplasmic subcellular compartment. Supporting this finding, DFF40/CAD overexpression allowed GBM cells to display oligonucleosomal DNA degradation after apoptotic challenge. Moreover, the analysis of histological slices from astrocytic tumors showed that DFF40/CAD immunoreactivity in tumoral GFAP-positive cells was markedly reduced when compared with nontumoral samples.

Conclusions. Our data highlight the low expression levels of DFF40/CAD and the absence of DNA laddering as common molecular traits in GBM. These findings could be of major importance for understanding the malignant behavior of remaining tumor cells after radiochemotherapy.

Keywords: apoptosis, caspase-dependent DNase (DFF40/CAD), caspase-dependent cell death, glioblastoma, oligonucleosomal DNA degradation.

Gliomas, tumors arising from glial cells, represent 80% of malignant brain tumors.[1] According to their aggressiveness, the World Health Organization (WHO) classifies gliomas into 4 different grades (I–IV).[2,3] Grades I and II are grouped together as low-grade gliomas and grades III and IV as high-grade gliomas. Glioblastoma (GBM) or grade IV astrocytoma represents

Received 11 June 2015; accepted 2 December 2015

the most frequent and aggressive brain tumor. Microvascular proliferation and necrotic areas, often surrounded by radially oriented, densely packed, small fusiform glial cells in a pseudopalisading pattern, are considered histopathological hallmarks of GBM.[4] Although the origin of the necrotic areas in GBM remains controversial, some evidence points to abortive apoptotic processes as a potential cause driving GBM cells to necrosis.[5–7,8] Apoptosis, triggered by the activation of caspases (reviewed in[9]), is characterized by oligonucleosomal DNA fragmentation. Executioner caspase-3, -6, and -7 trigger apoptotic hydrolysis of DNA through activation of DFF40/CAD (DNA fragmentation factor, 40-kDa subunit[10]/caspase-activated DNase[11]) endonuclease. In resting cells, DFF40/CAD is associated with its inhibitor, ICAD, which becomes processed and inactivated after caspase-3-mediated cleavage.[10,12,13] Since activation of caspase-3 mainly occurs at the cytosol, the ICAD/CAD complex should be located at this subcellular compartment to become properly activated.[14]

Here, we treated human GBM-derived cells with staurosporine, a strong apoptotic insult. None of the staurosporine-treated GBM cells displayed oligonucleosomal DNA degradation, not even those in which caspases were correctly activated. All GBM cells showed limited cytosolic DFF40/CAD protein levels. Thus, the sole overexpression of the endonuclease was sufficient to enable injured GBM cells to display oligonucleosomal DNA fragmentation. Finally, GFAP-positive cells from patients affected with astrocytic tumors showed reduced DFF40/CAD immunoreactivity compared with GFAP-positive cells from nontumoral brain tissue. Altogether, our results demonstrate that GBM cells are unable to complete classical apoptosis because of limited cytosolic DFF40/CAD protein levels.

Materials and Methods

Reagents

Pan-caspase inhibitor q-VD-OPh was purchased from MP Biomedicals Europe. All chemicals were obtained from Sigma-Aldrich unless otherwise indicated. Antibodies used in this study are summarized in Supplementary Table S1.

Cell Lines and Culture Procedures

Human GBM-derived cell lines A172, LN-18, LN-229, U87-MG (ATCC, 2010), T98G (ATCC, 2004), and U251-MG (ECACC, 2013), as well as human neuroblastoma-derived SH-SY5Y (ATCC, 2009), were used up to 2 months after having been thawed. Cells were routinely grown in Dulbecco's modified Eagle's medium supplemented with 100 U/mL penicillin, 100 μg/mL streptomycin, and 10% heat-inactivated fetal bovine serum (Invitrogen). Cells were maintained at 37°C in a saturated-humidity atmosphere containing 95% air and 5% CO_2.

Patient-derived Glioblastoma Cell Cultures

Patient-derived noncommercial GBM cells #30 (passages 8–17), #35 (passages 16–19), #45 (passages 11–12), and #52 (passages 9–16) were previously obtained.[15] For obtaining cells #04, tumor sample (around 1 cm^3) was rinsed with phosphate-buffered saline (PBS), mechanically dissociated into pieces, and incubated with trypsin (0.025% trypsin and 0.01% EDTA [Life Technologies]) for 3 minutes at 37°C. The cellular suspension was carefully recovered without disturbing non-dissociated aggregates and mixed with complete medium. The trypsinization process was repeated 4 times with the remaining pellets. Cellular suspensions were centrifuged at $200 \times g$ for 5 minutes and incubated in Red Blood Lysis Buffer (155 mM NH_4Cl, 12 mM $NaHCO_3$, 0.1 mM EDTA) for 10 minutes. After centrifugation, the cells were resuspended and plated in a 25 cm^2 flask. Clinical data from all participants are summarized in Supplementary Table S2.

Trypan Blue Exclusion Assay

Trypan blue exclusion assay was performed as previously established.[16] Cell death was expressed as a percentage of blue-positive (dead) over total (blue-positive and blue-negative) cells.

Oligonucleosomal DNA Degradation Analysis

Oligonucleosomal DNA degradation analysis was carried out as previously described.[17]

DEVD-directed Caspase-like Activity

Quantitative DEVD-directed activity assay was performed as previously described.[18]

Protein Extractions and Western Blotting

Cells were detached, pelleted at $500 \times g$ for 5 minutes, and washed once with PBS. Cells were lysed with Igepal buffer (50 mm Tris-HCl, pH 6.8, 1 mm EDTA, 150 mm NaCl, 1% Igepal CA-630, 1X protease inhibitor cocktail) for cytosolic protein extracts or SET buffer (10 mm Tris-HCl, pH 6.8, 150 mm NaCl, 1 mm EDTA, 1% SDS) to obtain total protein extracts as described previously.[18] Otherwise, cytosolic, nucleoplasmic, and chromatin-enriched fractions were obtained as previously established.[14] Protein extracts were loaded into SDS-polyacrylamide gels, electrophoresed, and electrotransferred. Membranes were incubated with the appropriate primary and secondary antibodies. Finally, membranes were stained with naphthol blue, allowed to dry, and scanned. Image J software was used for the quantification analysis of Western blots in Supplementary Table S3 and Supplementary Fig. S2.

Transfection of DFF40/CAD

Cells were transfected with the eukaryotic expression vector pcDNA3 (Invitrogen) carrying DFF40/CAD cDNA or with the empty vector[16] by using Lipofectamine 2000 Reagent (Invitrogen) and Attractene Transfection Reagent (Qiagen) for commercial and noncommercial cells, respectively, according to the manufacturer's instructions.

Hematoxylin and Eosin Staining

Immediately after surgery, tumor samples were fixed with formalin and embedded in paraffin blocks. Next, slices of 5-μm thick were sectioned and conventionally stained with hematoxylin-eosin according to Hospital de Bellvitge's standard protocols.

Immunofluorescence in Paraffin-embedded Tissue Sections

Paraffin-embedded tissue sections (5 μm thick) underwent dewaxing and rehydration. For antigen retrieval, slices were heated in a microwave (250 W) oven for 8 minutes in a buffer containing 10 mM sodium citrate (pH 6.0) and 0.05% Tween-20. After preincubation with blocking solution (5% normal goat serum and 0.02% triton X-100 in PBS), slices were incubated with antibodies against DFF40/CAD and GFAP (overnight at 4°C) and then with the appropriate secondary antibodies in the presence of 1 μg/mL 4,6-diamidino-2-phenylindole (DAPI). Finally, sections were mounted with an aqueous mounting medium (FluorSave reagent, Calbiochem) and examined using a laser confocal microscope (Zeiss LSM 700, Carl Zeiss) and the specific confocal software (ZEN, Carl Zeiss). For quantification of DFF40/CAD signal, images were analyzed with IMARIS 8 software. DFF40/CAD immunolabeling was evaluated only in GFAP-positive areas.

Immunofluorescence of Thick Floating Sections in Tumoral and Nontumoral Tissues

Sections of 60 μm thick from nontumoral (individual without neoplastic disease) human brain cortex or GBM were processed for high-resolution confocal analysis and 3D reconstruction. The immunofluorescence protocol in thick floating sections, laser scanning settings, and rendering have been previously described.[19,20] 3D image rotations were rendered with α-blending software IllucidaFX (Illucida LLC).

Statistical Analysis

A publicly available dataset containing 284 samples (including gliomas and nontumoral brain [R2: microarray analysis and visualization platform http://r2.amc.nl]) (Tumor Glioma French database, GSE16011)[21] was used to analyze DFF40/CAD mRNA levels. The results obtained are shown in Supplementary Fig. S4. The influence of DFF40/CAD mRNA expression levels on the overall survival of GBM patients (graphed in Supplementary Fig. S3) was assessed by using The Cancer Genome Atlas glioblastoma dataset ($n = 540$). Univariate analysis was performed by constructing probability curves according to the Kaplan-Meier method and comparing them using the log-rank test. Multiple comparisons between groups in Fig. 5C and Supplementary Figs. S4 and S5 were performed using 1-way ANOVA and Tukey's test as post hoc test.

Study Approval

Prior to their participation in the study, all participants provided informed consent in accordance with the Hospital Universitari de Bellvitge Ethics Committee. Paraffin tissues were obtained from the archives of the Institute of Neuropathology, Hospital Universitari de Bellvitge, according to the tissue bank regulations of the same center and were used after approval by the local regulatory authorities. The study involving thick floating sections was carried out according to the approved protocols, and the institutional authorization of the Scientific & Ethics Committee of the Consorci Hospital General Universitari de València and written informed consent were obtained from all participants and/or their relatives.

Results

Glioblastoma-derived Cells Undergo Caspase-dependent Cell Death in the Absence of Oligonucleosomal DNA Degradation After Staurosporine Treatment

We have recently reported that GBM-derived LN-18 cells undergo caspase-dependent cell death without showing oligonucleosomal DNA fragmentation after challenge with apoptotic stimuli.[18] Hence, we asked whether this behavior was also shared by other GBM-derived cells. Once it was corroborated that staurosporine provoked cytotoxicity in other well-established GBM-derived cells (Fig. 1A), DNA integrity was analyzed. As shown in Fig. 1B, none of the GBM-derived cell lines employed showed DNA laddering upon staurosporine treatment; thus, corroborating this constituted a common feature among GBM-derived cell lines rather than a specific trait of LN-18 cells. Since the absence of DNA laddering could be explained by a lack in caspase activation, we analyzed whether GBM cells could activate these proteases after staurosporine challenge. DEVD-AFC fluorogenic peptide cleavage indicated caspase-like activity in all staurosporine-treated GBM cells (Supplementary Fig. S1). Moreover, the detection of caspase-mediated p120 (from α-fodrin cleavage), p47/37 (from lamin A/C cleavage), and p17 (from co-chaperone p23 cleavage) fragments by Western blot confirmed the activation of caspases-3, -6, and -7, respectively, after staurosporine treatment (Fig. 1C). Accordingly, the addition of the pan-caspase inhibitor q-VD-OPh to the culture media prevented both the appearance of the above-mentioned caspase-mediated fragments (Fig. 1C) and the cytotoxicity induced by the alkaloid (Fig. 1F). Thus, the lack of DNA laddering in injured GBM-derived cell lines was not due to a deficiency in caspase activation but was more likely due to downstream impairment in the hydrolysis of their genomic content.

Since repeated in vitro subcultured cancer cell lines often differ from the original primary human tumors,[22–25] we extended our results to patient-derived noncommercial GBM cells with a reduced number of cell passages in culture (< 20). The addition of staurosporine to the culture media of these cells (#04, #30, #35, #45, and #52) was also unable to induce DNA laddering (Fig. 1D) despite the high cytotoxicity observed (Fig. 1G). After treatment, GBM-derived #04, #35, and #52 cells showed activation of caspase-3, -6, and -7 as inferred from the detection of their specific caspase-mediated proteolytic fragments (Fig. 1E). In #30 cells, staurosporine induced the cleavage of α-fodrin and co-chaperone p23 but not lamin A/C, pointing to a particular impairment in caspase-6 activation (Fig. 1E). In #45 cells, the caspase-triggered cleavage of these 3 specific substrates was completely absent. In agreement with these results, the addition of q-VD-OPh to the culture media successfully avoided staurosporine-induced cytotoxicity in #04, #30, #35, and #52 cells (Fig. 1G).

Glioblastoma Cells Exhibit Low Levels of Cytosolic DFF40/CAD Albeit Caspase-3/ICAD/CAD Axis Is Correctly Activated

During apoptosis, caspase-3 cleaves ICAD, allowing DFF40/CAD endonuclease release and activation.[10,13] As shown in Fig. 2A and B, GBM-derived cells showed caspase-3, ICAD (long [$ICAD_L$] and short [$ICAD_S$] isoforms), and DFF40/CAD

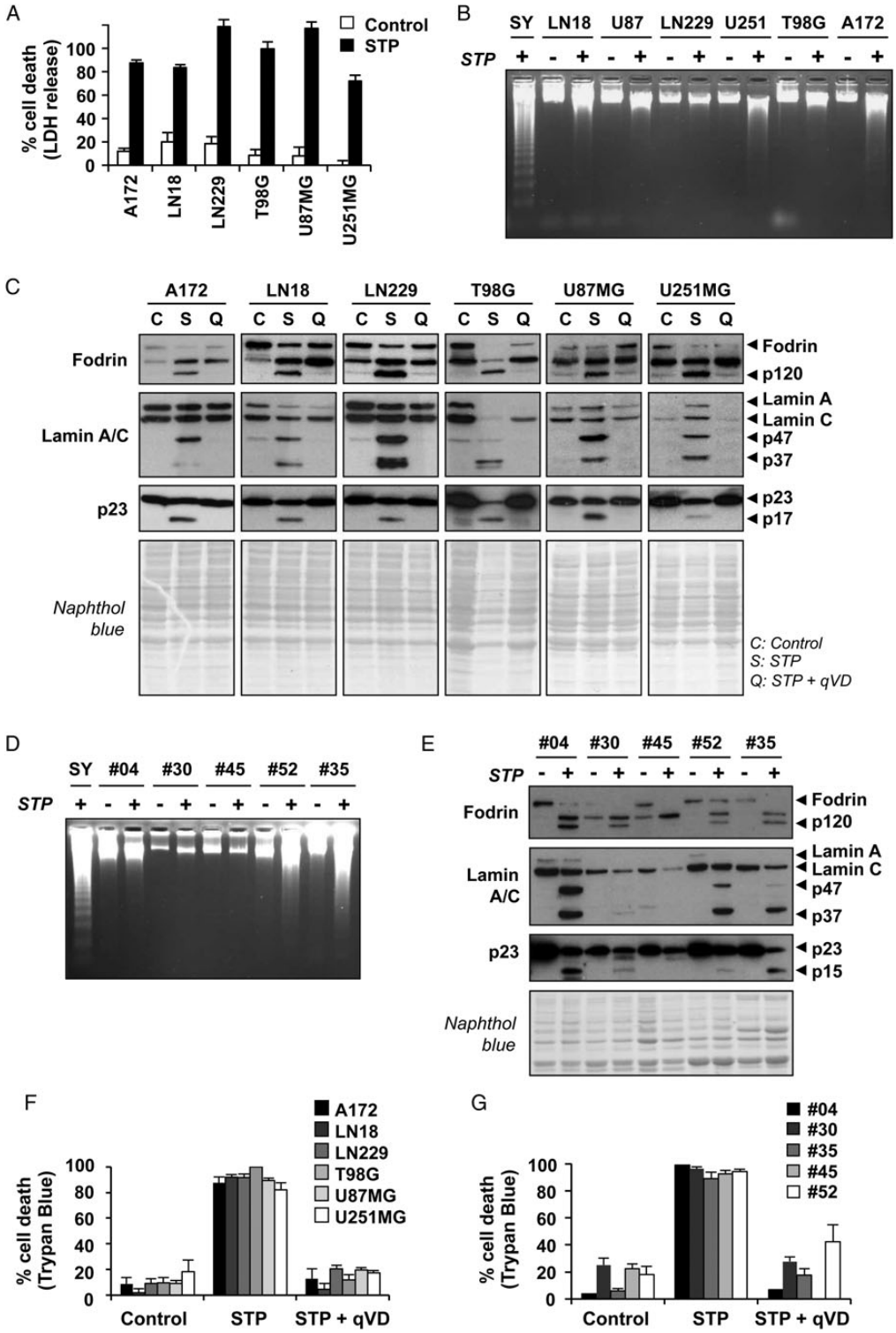

Fig. 1. Glioblastoma (GBM) cells are unable to hydrolyze DNA into oligonucleosome-sized fragments during staurosporine-triggered apoptosis. Cells were treated with 1 μM staurosporine (STP, S or +), with 1 μM staurosporine plus 10 μM q-VD-OPh (Q) or left untreated (Control, C or -) as indicated. (A) After 24 hours, cell death was evaluated by LDH release assay. Results are represented as the means ± SD ($n = 4$). (B and D) After 6 hours, DNA was extracted and electrophoresed. Staurosporine-treated human neuroblastoma-derived SH-SY5Y cells were used as proficient cells displaying oligonucleosomal DNA fragmentation. (C and E) After 6 hours, protein extracts were obtained, and immunoblots against fodrin, lamin A/C, and p23 co-chaperone were carried out to assess the activation of caspases-3, -6, and -7, respectively (35 μg). Naphthol blue staining of membranes was used to demonstrate equal loading. (F and G) Trypan blue assay was performed after 24 hours (or 48 h in the case of #52 cells). The graph represents the means ± SD of at least 300 cells ($n = 3$).

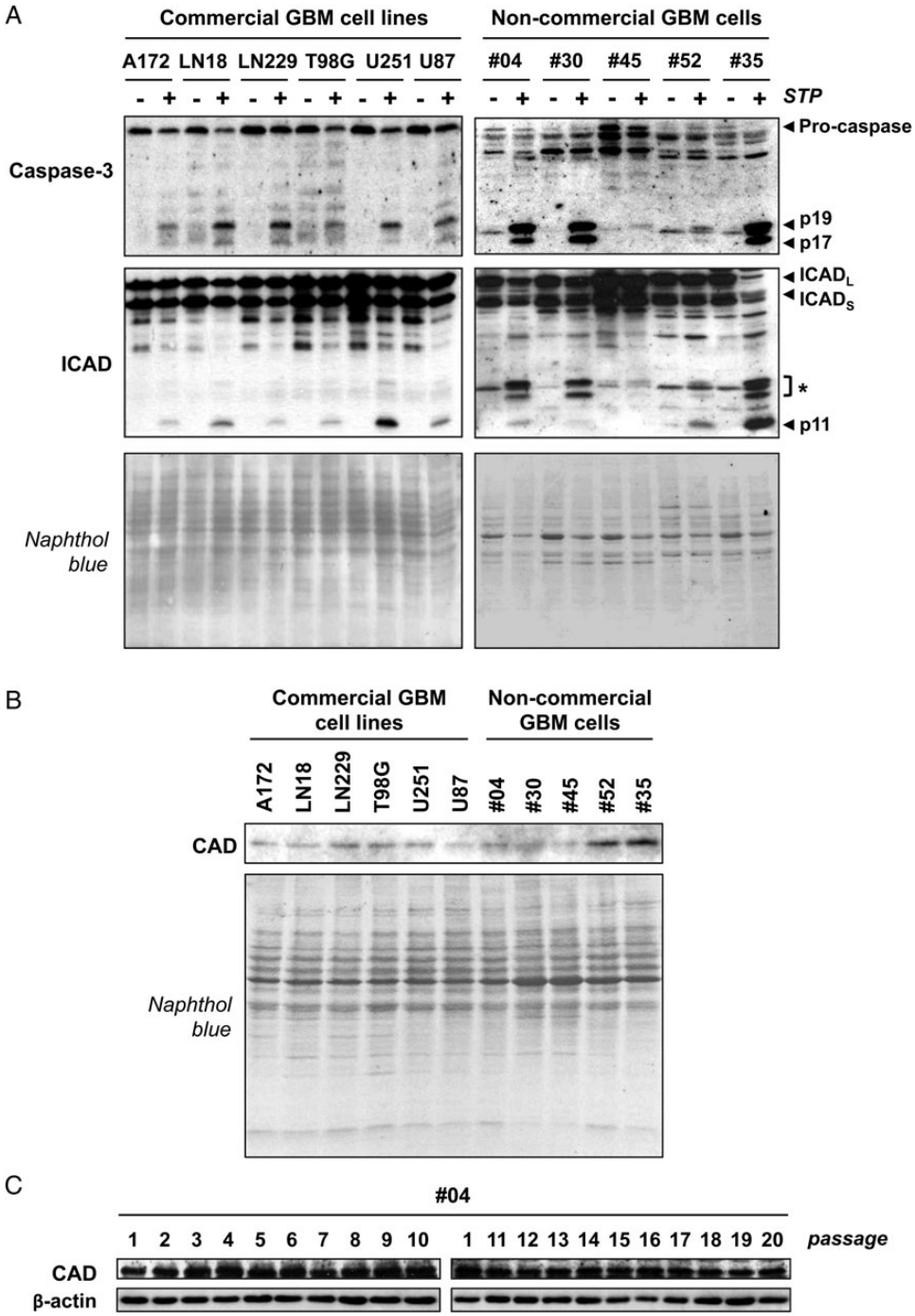

Fig. 2. Glioblastoma (GBM) cells show proper ICAD processing after staurosporine treatment but display low DFF40/CAD protein levels. (A) Cells were treated with 1 μM staurosporine (STP, +) or left untreated (−) for 6 hours. Protein extracts were obtained, and immunoblots against caspase-3 and ICAD were performed (35 μg). (B) DFF40/CAD total protein levels were assessed (35 μg). Naphthol blue staining of membranes was used to demonstrate equal loading in A and B. (C) Patient-derived GBM #04 cells were cultured from its dissociation (passage 1) to passage 20. Protein extracts were obtained from every passage, and immunoblots against DFF40/CAD were performed (25 μg). Anti-β-actin was used as loading control. *: bands from a previous blot.

expression. Moreover, staurosporine-treated cells undergoing caspase-3 activation also displayed caspase-3-mediated ICAD processing (Fig. 2A). Since the presence of serum can induce pronounced phenotypic and genotypic differences in GBM cells from passage 3,[25] we evaluated DFF40/CAD protein expression at different passages. As shown in Fig. 2C, DFF40/CAD protein levels remained stable over cell culture for at least 20 passages (Fig. 2C).

Due to the relevance of DFF40/CAD cytosolic pool for oligonucleosomal DNA hydrolysis during apoptosis,[14] we evaluated caspase-3, ICAD, and DFF40/CAD intracellular distribution in cytosolic, nucleoplasmic, and chromatin-enriched fractions. In untreated cells, procaspase-3 and ICAD were detected at both cytosolic and nucleoplasmic fractions. However, despite certain amounts being observed at the cytosol, DFF40/CAD was mainly found at the nucleoplasmic fraction (Fig. 3). Indeed, the cytoplasmic/nucleoplasmic DFF40/CAD ratio was lower than 1 in all GBM cells, contrary to that observed in apoptotic-proficient neuroblastoma-derived SH-SY5Y cells (Supplementary Table. S3). After apoptotic insult, caspase-3 active fragments and ICAD processing were observed at the cytosolic fraction, being only slightly detected at the nucleoplasmic and completely absent at the chromatin-enriched fractions (Fig. 3). After staurosporine treatment, cytosolic DFF40/CAD disappeared, nucleoplasmic DFF40/CAD remained unaltered, and certain levels of the endonuclease appeared in the chromatin-enriched fraction (Fig. 3). So far, these results indicated that DFF40/CAD subcellular localization in GBM cells (mostly nucleoplasmic) did not match with the subcellular compartment (cytosol) in which caspase-3 activation and ICAD fragmentation occurred preferentially.

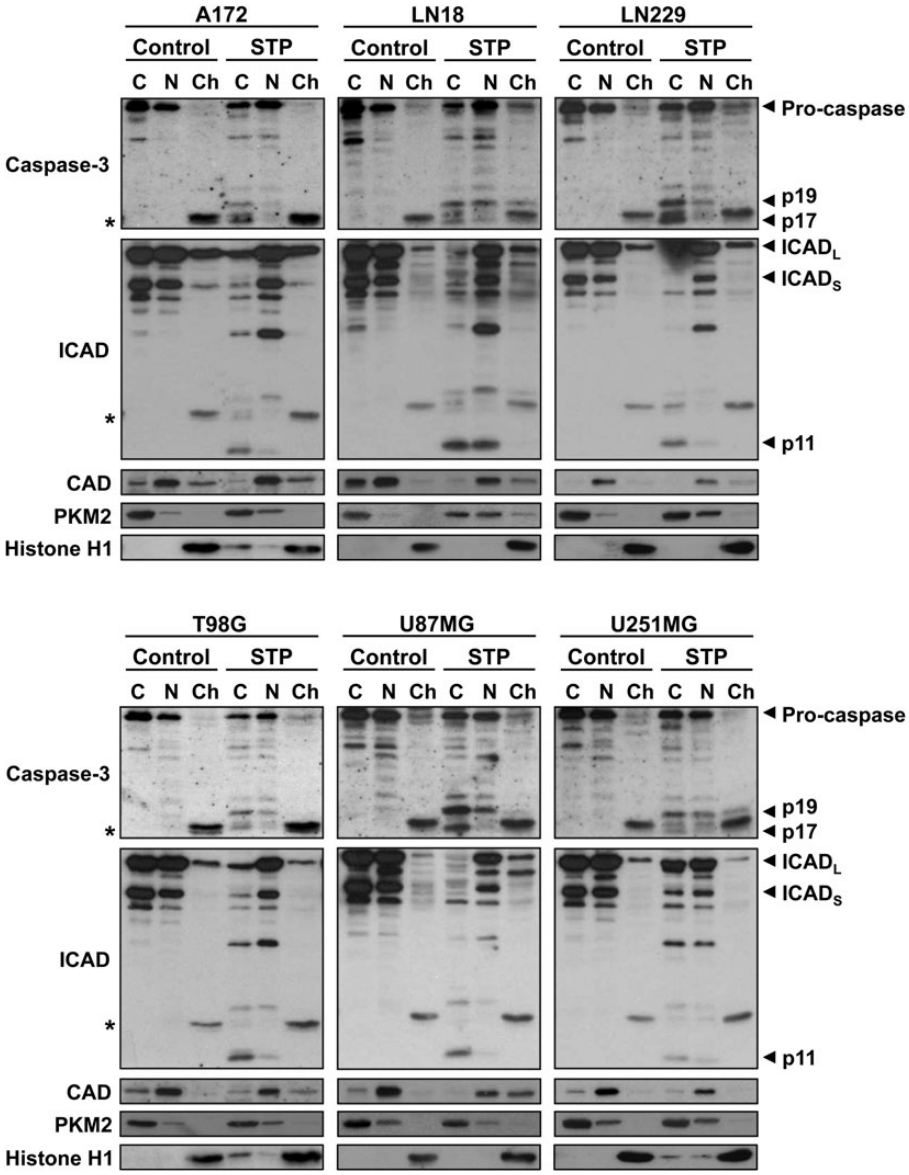

Fig. 3. DFF40/CAD is mainly located at the nucleoplasmic fraction rather than the cytosolic fraction in glioblastoma (GBM) cells. Cells were treated with staurosporine for 6 hours (STP) or left untreated (control); cytosolic (C), nucleoplasmic (N), and chromatin-enriched (Ch) fractions were obtained. Caspase-3, ICAD, and DFF40/CAD were assessed through Western blot in all fractions. PKM2 and histone H1 were used as markers of cytosolic and chromatin-enriched fractions, respectively. Note that DFF40/CAD mobilizes from the cytosolic fraction to the chromatin-enriched fraction after treatment. *: unspecific bands.

DFF40/CAD Overexpression Allows Injured Glioblastoma Cells to Degrade DNA Into Oligonucleosome-sized Fragments

Next, we overexpressed the endonuclease in GBM-derived cells. DFF40/CAD overexpression enabled GBM cells to hydrolyze their DNA into oligonucleosome-sized pieces after staurosporine treatment (Fig. 4), correlating with an increase in the cytoplasmic levels of DFF40/CAD (Supplementary Fig. S2). However, as already observed in nontransfected cells, the cytosolic/nucleoplasmic DFF40/CAD ratio in GBM-transfected cells was still lower than 1 (Supplementary Fig. S2). Therefore, the defect of GBM cells in displaying DNA laddering after apoptotic stimulus seemed to be linked to the low DFF40/CAD protein levels, particularly in the cytosolic compartment.

DFF40/CAD Is Barely Detected in Histological Slices From Glioblastoma-affected Participants

Next, we carried out immunohistofluorescence against DFF40/CAD in histological samples from patients #04, #30, #45, and #52. All GBM slices showed low immunoreactivity for DFF40/CAD (Supplementary Fig. S5). By taking advantage of hematoxylin-eosin staining and GFAP immunoreactivity, we detected 3 differential histopathological areas in patient #35. One of these was characterized by high-grade glial proliferation with marked pleomorphism, mitosis, necrotic areas, and microvascular proliferation[2] (Fig. 5A left), few giant cells, and low GFAP immunoreactivity[26] (Fig. 5A right). The other 2 regions, which corresponded to adjacent cerebral cortex, showed no signs of high-grade glial proliferation. One of them exhibited low-grade glial proliferation (intermediate GFAP immunoreactivity[26] without signs of microvascular proliferation or necrosis[2]) intermingled with reactive gliosis (high GFAP immunoreactivity[26]). The other area was classified as a tumor-free piece of cortex, according to the high-level organization of the cellular architecture and the lack of anaplasia, nuclear atypia, cellular pleomorphism, and mitotic activity[2] (Fig. 5A, left). In this tumor-free region, most GFAP-positive cells exhibited high DFF40/CAD immunoreactivity (Fig. 5B and C). However, GFAP-positive cells did not harbor immunoreactivity for anti-DFF40/CAD antibody in the high-grade tumoral region. Interestingly, the low-grade tumoral portion contained areas where DFF40/CAD immunoreactivity was similar to that observed in the tumor-free section and others in which the signal was lower (Fig. 5B and C). At that point, we analyzed DFF40/CAD in nontumoral samples. Non-neoplastic cortex, showing well-structured GFAP-positive cells, displayed high levels of DFF40/CAD labeling (Fig. 6A and B). This signal contrasted with the noticeably reduced immunostaining observed in the tumorigenic areas from GBM. In the core areas of the tumor, as evidenced by a marked cellularity, aberrant mitosis, and gemistocytic-like GFAP-positive cells, the labeling for DFF40/

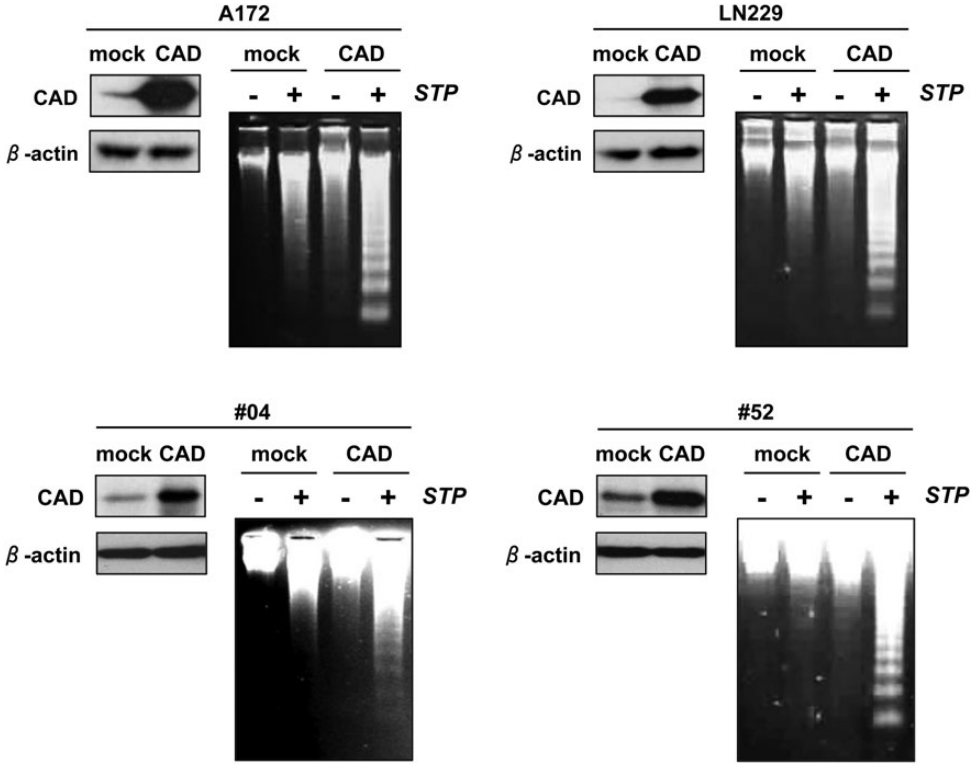

Fig. 4. DFF40/CAD overexpression allows apoptotic glioblastoma (GBM) cells to hydrolyze DNA into oligonucleosome-sized fragments. Cells transfected with a eukaryotic expression vector carrying the human DFF40/CAD (CAD) or with the empty vector (mock) were treated with 1 μM staurosporine (+) or left untreated (−). Western blot against DFF40/CAD was performed to corroborate the overexpression of the endonuclease in untreated cells. β-actin was used as loading control. After 6 hours of treatment, DNA was extracted and electrophoresed. Note that DNA laddering only appears in staurosporine-treated GBM cells that overexpress DFF40/CAD.

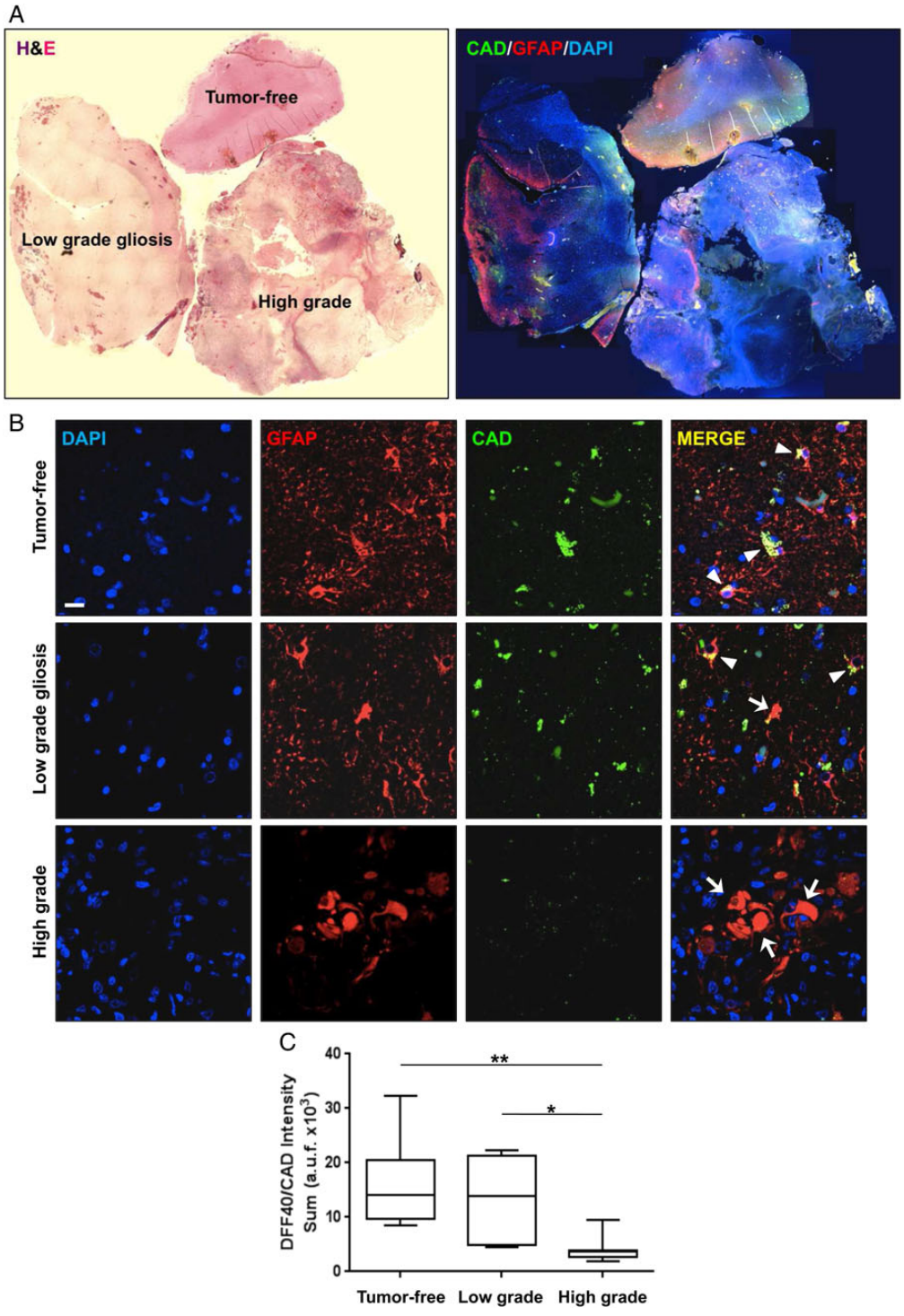

Fig. 5. DFF40/CAD immunoreactivity in a tumoral area exhibiting high-grade glial proliferation is reduced compared with the signal observed in a tumor-free region from the same participant. (A) Hematoxylin and eosin (H&E) staining (left) or immunostaining against DFF40/CAD (green) and GFAP (red), and DAPI nuclear staining (blue) (right) were performed in paraffin-embedded slices from participant #35. Images shown are composites of 150 microphotographs for H&E staining or 303 microphotographs, 101 in each color, for immunohistofluorescence. Note the 3 histopathologically differentiated regions observed in the slice and classified as "high grade," "low grade gliosis," and "tumor-free." Note that hemorrhagic areas, probably caused by the surgery, were unspecifically recognized by the DFF40/CAD antibody. (B) Representative confocal scanning images from each condition are shown. Scale bar = 10 μm. Arrowheads indicate GFAP-positive DFF40/CAD-positive cells. Arrows indicate GFAP-positive DFF40/CAD-negative cells. (C) Microphotographs from each histopathological region were processed with Imaris 8.1 software, and the intensity sum from the channel corresponding to DFF40/CAD signal was calculated. Graph represents the mean of arbitrary units of fluorescence (a.u.f.) ± SD ($n = 10$). * = $\alpha < 0.05$; ** = $\alpha < 0.01$.

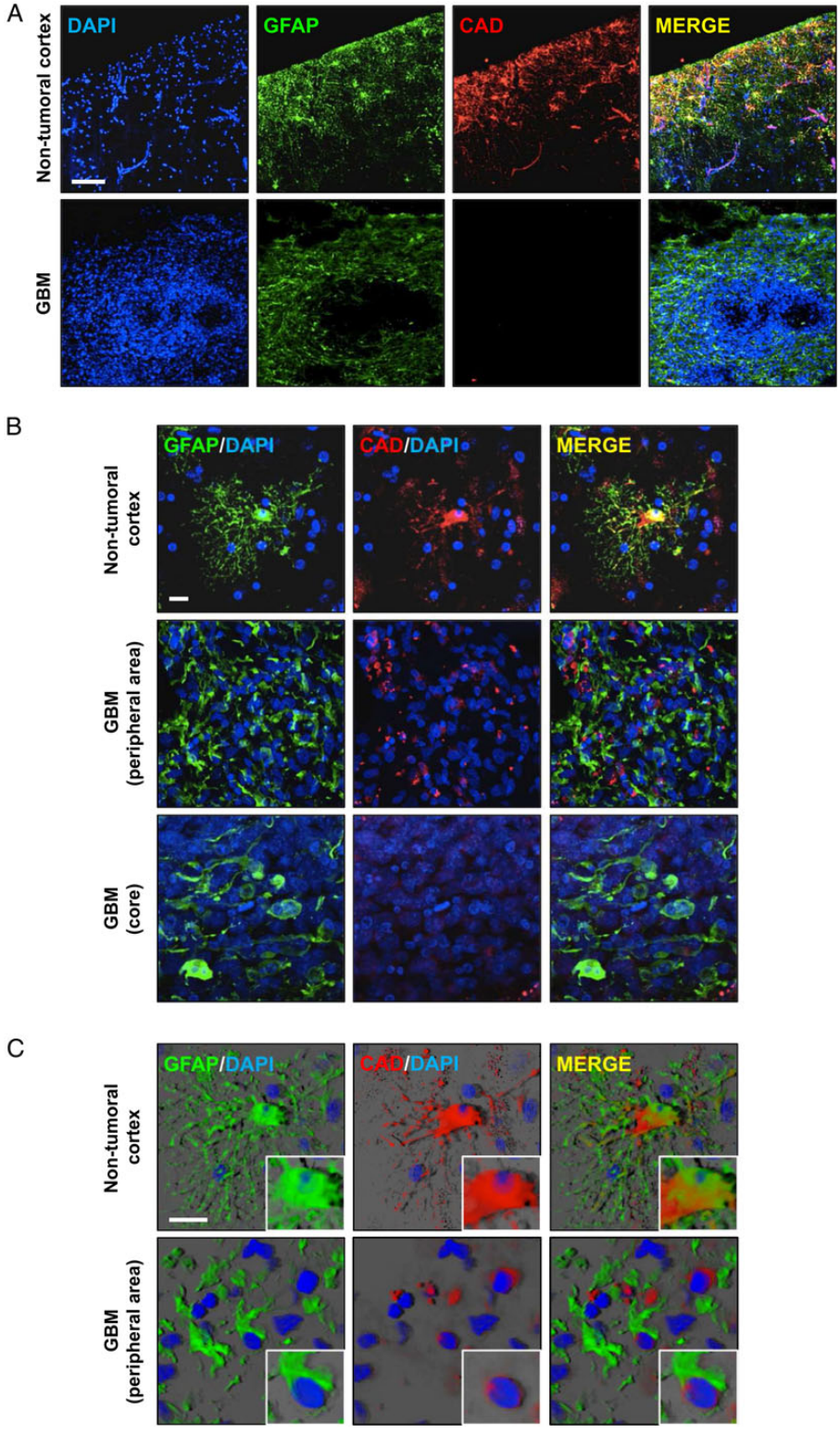

Fig. 6. Histological slices from glioblastoma (GBM) patients display less cytosolic DFF40/CAD immunoreactivity than nontumoral samples; 60 μm-thick sections from a nontumoral brain or neoplastic GBM cortex were immunostained with specific antibodies against DFF40/CAD (red) and GFAP (green), and DAPI (blue). Representative confocal scanning images from each condition are shown. (A) Panoramic views of the histological slices. (B) Detailed microphotographs showing GFAP-positive cells. (C) Confocal images from B, processed with a 3D rendering software are shown. In B and C, the microphotographs from DFF40/CAD immunostaining in the neoplastic tissue were obtained under a laser excitation 2 points higher than that used for the nontumoral cortex. Scale bars: A = 100 μm; B and C = 10 μm.

CAD was lower or even absent (Fig. 6A and B). Moreover, this reduced DFF40/CAD immunostaining in GFAP-positive tumoral cells localized at the perinuclear space, which was in sharp contrast with the strong cytosolic signal observed in GFAP-positive cells from nontumoral human cortex (Fig. 6C). Altogether, these results pointed the limited expression of DFF40/CAD in the cytosol as the major biochemical trait shared by GBM cells, supporting the lack of DNA laddering during caspase-dependent cell death.

Discussion

Here we stress that GBM-derived cells do not display oligonucleosomal DNA degradation after caspase-dependent apoptotic insult. This defect relies on the subcellular localization of DFF40/CAD endonuclease. To be properly activated, DFF40/CAD should reside in the same subcellular compartment (cytosol) where caspase-3 and ICAD are processed.[14] In GBM cells, DFF40/CAD accumulates at the nucleoplasmic fraction; albeit, caspase-3 and ICAD are mainly cytosolic. Moreover, DFF40/CAD-overexpressing cells still accumulate the endonuclease preferentially at the nucleus, revealing an intrinsic cellular defect that retains DFF40/CAD at the cytosol. DFF40/CAD nuclear import is regulated by interaction of the importin α/β-heterodimer with the C-terminus from both DFF40/CAD and ICAD.[27] The importin-α isoform expression is upregulated in GBM cells,[28] which could explain the nuclear accumulation of DFF40/CAD. Interestingly, upregulation of the gene encoding importin α (KPNA2) is associated with poor prognosis in astrocytomas.[28] Low mRNA levels of DFF40/CAD also correlate with worse overall survival in GBM patients (Supplementary Fig. S3). Overall, these findings suggest that either improper DFF40/CAD nuclear accumulation or low DFF40/CAD protein expression (as a consequence of low mRNA levels) could affect tumor progression. On the other hand, when analyzing the Tumor Glioma French dataset (GSE16011),[21] no significant differences are observed in DFF40/CAD mRNA levels between astrocytic tumors and nontumoral brain samples (Supplementary Fig. S4). This suggests that dysregulation of the endonuclease in astrocytomas might be mainly due to (post)translational mechanisms rather than genetic or epigenetic control.

Besides its role as apoptotic endonuclease, the absence of DFF40/CAD has been linked to genomic instability and tumorigenesis.[29] We have observed that DFF40/CAD downregulation is not a genetic event in GBM cells but is instead a translation-regulated event. It can then be argued that the loss of DFF40/CAD could be an adaptive biochemical process facilitating genomic instability in response to not yet characterized extracellular stresses. This allows tumoral cells to acquire mutations that could contribute to aggressiveness and drug-resistant phenotypes in GBM.[29–31] On the other hand, since reduced DFF40/CAD immunostaining is observed not only in GBM, but also in grades II and III astrocytomas (Supplementary Fig. S5), the loss of DFF40/CAD expression may reflect a molecular peculiarity already present in a common premalignant cell precursor. Although DFF40/CAD-null mice do not develop tumors spontaneously, they exhibit higher cancer susceptibility when exposed to carcinogens or genotoxic stress.[29] Likewise, genetically modified mice lacking only one tumor-suppressor gene, such as *gadd45*, *p16INK4a*, *chk2*, or *ku80*, do not develop tumors spontaneously[32–35]; however, when these genes are knocked out in genetically modified mice that develop cancer spontaneously, tumors arise at a higher frequency.[33,35] On theoretical grounds, it is exciting to speculate that the DFF40/CAD downregulation observed in GBM cells may be intimately related to gliomagenesis and thus drive the initial steps of tumoral transformation.[29,36] In this regard, progressive loss of DFF40/CAD immunoreactivity is observed in histological slices being more pronounced in the core of the tumor, indicating that DFF40/CAD expression correlates inversely with histopathological malignancy grade. These findings were clearly evident in participant #35, in whom 3 distinct histopathological areas could be distinguished including nontumoral, low-grade gliosis, and high-grade glial proliferation.

In any case, the loss of DFF40/CAD emerges as a newly discovered molecular alteration that is common to astrocytomas. Consequently, injured GBM cells are unable to display DNA laddering after apoptotic insult. To the best of our knowledge, this is the first report of such homogeneous cytotoxic behavior within the same class of tumors. This fact is particularly relevant when considering the high biochemical and molecular heterogeneity that characterizes GBM cells (reviewed in[31]). All GBM-derived cells employed in this study lacked DNA laddering after apoptotic insult regardless of the particular mutations exhibited.[37] An interesting question arising from these findings turns around on the potential (dis)advantages derived from an incomplete degradation of the genomic content during caspase-dependent cell death. It has always been assumed that proper DNA degradation into oligonucleosome-sized pieces would facilitate phagocytosis of packaged chromatin and thus minimizing the risk of oncogenic transfer.[38] We have recently reported that GBM-derived LN-18 cells lost nuclear envelope integrity after apoptotic insult.[18] This fact, together with the necrotic biology of GBM, makes it reasonable to consider that the genomic fragments generated during caspase-dependent cell death could be found in either the cytoplasm or outside the cell. Supporting this, the amount of long, but not small, DNA fragments in cerebrospinal fluid from glioma patients is approximately twice that found in healthy individuals.[39] It has also been reported that oxidized DNA circulating in the serum could favor survival and stress resistance of the remaining malignant cells in different kinds of tumors.[40] Since reduced DFF40/CAD immunostaining is observed in both GBM and grades II and III astrocytomas, we might assume that these tumors could potentially release their genetic content independent of their clinical grade. However, GBM shows increased levels of oxidative DNA damage (by 8-oxoguanine) compared with lower-grade astrocytomas and normal brain.[41] Therefore, it is plausible that not just DNA release, but the release of oxidized DNA, constitute an important aspect for understanding the clinical differences observed between GBM and other astrocytomas. In this sense, either spontaneously- or therapeutically-injured GBM cells are a potential source of oxidized DNA, which could impair the effectiveness of current therapies. Our results show that DFF40/CAD overexpression allows GBM cells to fragment DNA into small pieces after apoptotic insult. Therefore, we hypothesize that proper endogenous DFF40/CAD activity would maximize the amount of DNA fragments packaged into closed, blebbed apoptotic bodies, minimizing the risk of

DNA spread and preventing oxidized DNA-driven radiochemotherapy resistance.

In summary, we identified the improper expression of DFF40/CAD endonuclease and the subsequent lack of oligonucleosomal DNA fragmentation as being the unifying molecular signatures of this highly heterogeneous disease.[42,43] Drs. T. Ozawa and E. C. Holland wrote "… Rather than narrowly treating specific mutations and subtypes, we should be looking for therapies that address the biology of gliomas as a whole. We should target the things that unify this disease rather than those that appear to subdivide it."[44] Accordingly, our findings could be of the utmost relevance. Indeed, because DFF40/CAD deficiency improves cell survival after radiation[29] and the radiochemotherapy-induced spread of oxidized DNA from dying cells could diminish the efficacy of treatment,[40] our results question if the current therapeutic approaches are optimal for treating GBM.

Supplementary Material

Supplementary material is available at *Neuro-Oncology Journal* online (http://neuro-oncology.oxfordjournals.org/).

Acknowledgments

We thank all other members of the labs and hospital departments for their support. We specially thank Dr. M. Garcia-Belinchón for her helpful criticisms.

Funding

This work was supported by "Ministerio de Economía y Competitividad/Fondo Europeo de Desarrollo Regional" SAF2012-31485 and "Agència de Gestió d'Ajuts Universitaris" (Generalitat de Catalunya) SGR2014-1609 grants to V.J.Y.; "Ministerio de Ciencia e Innovación" RYC2010-06729 and "Ministerio de Economía y Competitividad/Fondo Europeo de Desarrollo Regional" SAF2010-21274 and SAF2013-45178-P grants to C.B.; "Formación de Personal Universitario" fellow from "Ministerio de Ciencia e Innovación" to M.S.-O.; and "Agència de Gestió d'Ajuts Universitaris" (Generalitat de Catalunya) fellow to V.I.-G. V.J.Y. is under a "Retention of Research Talent" contract from "Programa Banco de Santander."

Conflict of interest statement. The authors disclose no potential conflicts of interest.

References

1. Ostrom QT, Gittleman H, Liao P, et al. CBTRUS statistical report: primary brain and central nervous system tumors diagnosed in the United States in 2007–2011. *Neuro Oncol*. 2014;16(Suppl 4):iv1–i63.
2. Louis DN, Ohgaki H, Wiestler OD, Cavenee WK, eds. *WHO Classification of Tumours of the Central Nervous System*. Lyon: IARC Press; 2007.
3. Louis DN, Ohgaki H, Wiestler OD, et al. The 2007 WHO classification of tumours of the central nervous system. *Acta Neuropathol*. 2007;114(2):97–109.
4. Rong Y, Durden DL, Van Meir EG, Brat DJ. 'Pseudopalisading' necrosis in glioblastoma: a familiar morphologic feature that links vascular pathology, hypoxia, and angiogenesis. *J Neuropathol Exp Neurol*. 2006;65(6):529–539.
5. Bell HS, Whittle IR, Walker M, Leaver HA, Wharton SB. The development of necrosis and apoptosis in glioma: experimental findings using spheroid culture systems. *Neuropathol Appl Neurobiol*. 2001;27(4):291–304.
6. Raza SM, Lang FF, Aggarwal BB, Fuller GN, Wildrick DM, Sawaya R. Necrosis and glioblastoma: a friend or a foe? A review and a hypothesis. *Neurosurgery*. 2002;51(1):2–12; discussion 12–13.
7. Stegh AH, Kim H, Bachoo RM, et al. Bcl2L12 inhibits post-mitochondrial apoptosis signaling in glioblastoma. *Genes Dev*. 2007;21(1):98–111.
8. Garcia-Belinchon M, Sanchez-Osuna M, Martinez-Escardo L, et al. An Early and Robust Activation of Caspases Heads Cells for a Regulated Form of Necrotic-like Cell Death. *J Biol Chem*. 2015;290(34):20841–20855.
9. Shalini S, Dorstyn L, Dawar S, Kumar S. Old, new and emerging functions of caspases. *Cell Death Differ*. 2015;22(4):526–539.
10. Liu X, Li P, Widlak P, et al. The 40-kDa subunit of DNA fragmentation factor induces DNA fragmentation and chromatin condensation during apoptosis. *Proc Natl Acad Sci USA*. 1998;95(15):8461–8466.
11. Enari M, Sakahira H, Yokoyama H, Okawa K, Iwamatsu A, Nagata S. A caspase-activated DNase that degrades DNA during apoptosis, and its inhibitor ICAD. *Nature*. 1998;391(6662):43–50.
12. Liu X, Zou H, Slaughter C, Wang X. DFF, a heterodimeric protein that functions downstream of caspase-3 to trigger DNA fragmentation during apoptosis. *Cell*. 1997;89(2):175–184.
13. Sakahira H, Enari M, Nagata S. Cleavage of CAD inhibitor in CAD activation and DNA degradation during apoptosis. *Nature*. 1998;391(6662):96–99.
14. Iglesias-Guimarais V, Gil-Guinon E, Gabernet G, et al. Apoptotic DNA degradation into oligonucleosomal fragments, but not apoptotic nuclear morphology, relies on a cytosolic pool of DFF40/CAD endonuclease. *J Biol Chem*. 2012;287(10):7766–7779.
15. Villalonga-Planells R, Coll-Mulet L, Martinez-Soler F, et al. Activation of p53 by nutlin-3a induces apoptosis and cellular senescence in human glioblastoma multiforme. *PloS One*. 2011;6(4):e18588.
16. Yuste VJ, Bayascas JR, Llecha N, Sanchez-Lopez I, Boix J, Comella JX. The absence of oligonucleosomal DNA fragmentation during apoptosis of IMR-5 neuroblastoma cells: disappearance of the caspase-activated DNase. *J Biol Chem*. 2001;276(25):22323–22331.
17. Boix J, Llecha N, Yuste VJ, Comella JX. Characterization of the cell death process induced by staurosporine in human neuroblastoma cell lines. *Neuropharmacology*. 1997;36(6):811–821.
18. Sanchez-Osuna M, Garcia-Belinchon M, Iglesias-Guimarais V, Gil-Guinon E, Casanelles E, Yuste VJ. Caspase-activated DNase is necessary and sufficient for oligonucleosomal DNA breakdown, but not for chromatin disassembly during caspase-dependent apoptosis of LN-18 glioblastoma cells. *J Biol Chem*. 2014;289(27):18752–18769.
19. Barcia C, Thomas CE, Curtin JF, et al. In vivo mature immunological synapses forming SMACs mediate clearance of virally infected astrocytes from the brain. *J Exp Med*. 2006;203(9):2095–2107.
20. Barcia C Jr., Gomez A, Gallego-Sanchez JM, et al. Infiltrating CTLs in human glioblastoma establish immunological synapses with tumorigenic cells. *Am J Pathol*. 2009;175(2):786–798.

21. Gravendeel LA, Kouwenhoven MC, Gevaert O, et al. Intrinsic gene expression profiles of gliomas are a better predictor of survival than histology. *Cancer Res*. 2009;69(23):9065–9072.
22. Hecht BK, Turc-Carel C, Chatel M, et al. Cytogenetics of malignant gliomas: I. The autosomes with reference to rearrangements. *Cancer Genet Cytogenet*. 1995;84(1):1–8.
23. Deschavanne PJ, Fertil B. A review of human cell radiosensitivity in vitro. *Int J Radiat Oncol Biol Phys*. 1996;34(1):251–266.
24. Pardal R, Clarke MF, Morrison SJ. Applying the principles of stem-cell biology to cancer. *Nat Rev Cancer*. 2003;3(12):895–902.
25. Lee J, Kotliarova S, Kotliarov Y, et al. Tumor stem cells derived from glioblastomas cultured in bFGF and EGF more closely mirror the phenotype and genotype of primary tumors than do serum-cultured cell lines. *Cancer Cell*. 2006;9(5):391–403.
26. Middeldorp J, Hol EM. GFAP in health and disease. *Prog Neurobiol*. 2011;93(3):421–443.
27. Neimanis S, Albig W, Doenecke D, Kahle J. Sequence elements in both subunits of the DNA fragmentation factor are essential for its nuclear transport. *J Biol Chem*. 2007;282(49):35821–35830.
28. Gousias K, Becker AJ, Simon M, Niehusmann P. Nuclear karyopherin a2: a novel biomarker for infiltrative astrocytomas. *J Neurooncol*. 2012;109(3):545–553.
29. Yan B, Wang H, Peng Y, et al. A unique role of the DNA fragmentation factor in maintaining genomic stability. *Proc Natl Acad Sci U S A*. 2006;103(5):1504–1509.
30. Yan B, Wang H, Wang H, et al. Apoptotic DNA fragmentation factor maintains chromosome stability in a P53-independent manner. *Oncogene*. 2006;25(39):5370–5376.
31. Morokoff A, Ng W, Gogos A, Kaye A. Molecular subtypes, stem cells and heterogeneity: Implications for personalised therapy in glioma. *J Clin Neurosci*. 2015;22(8):1219–1226.
32. Hollander MC, Sheikh MS, Bulavin DV, et al. Genomic instability in Gadd45a-deficient mice. *Nat Genet*. 1999;23(2):176–184.
33. Krimpenfort P, Quon KC, Mooi WJ, Loonstra A, Berns A. Loss of p16Ink4a confers susceptibility to metastatic melanoma in mice. *Nature*. 2001;413(6851):83–86.
34. Hirao A, Cheung A, Duncan G, et al. Chk2 is a tumor suppressor that regulates apoptosis in both an ataxia telangiectasia mutated (ATM)-dependent and an ATM-independent manner. *Mol Cell Biol*. 2002;22(18):6521–6532.
35. Difilippantonio MJ, Zhu J, Chen HT, et al. DNA repair protein Ku80 suppresses chromosomal aberrations and malignant transformation. *Nature*. 2000;404(6777):510–514.
36. Errami Y, Brim H, Oumouna-Benachour K, et al. ICAD deficiency in human colon cancer and predisposition to colon tumorigenesis: linkage to apoptosis resistance and genomic instability. *PloS One*. 2013;8(2):e57871.
37. Meléndez B, García-Claver A, Ruano Y, et al. Copy number alterations in glioma cell lines. In: Ghosh A, ed. *Glioma - Exploring Its Biology and Practical Relevance*. Rijeka, Croatia: InTech; 2011: 429–448. Available from Chapter 19 in http://www.intechopen.com/books/glioma-exploring-its-biology-and-practical-relevance.
38. Samejima K, Earnshaw WC. Trashing the genome: the role of nucleases during apoptosis. *Rev Mol Cell Biol Nat*. 2005;6(9):677–688.
39. Shi W, Lv C, Qi J, et al. Prognostic value of free DNA quantification in serum and cerebrospinal fluid in glioma patients. *J Mol Neurosci*. 2012;46(3):470–475.
40. Glebova K, Veiko N, Kostyuk S, Izhevskaya V, Baranova A. Oxidized extracellular DNA as a stress signal that may modify response to anticancer therapy. *Cancer Lett*. 2015;356(1):22–33.
41. Bartkova J, Hamerlik P, Stockhausen MT, et al. Replication stress and oxidative damage contribute to aberrant constitutive activation of DNA damage signalling in human gliomas. *Oncogene*. 2010;29(36):5095–5102.
42. Ene CI, Holland EC. Personalized medicine for gliomas. *Surg Neurol* Int. 2015;6(Suppl 1):S89–S95.
43. Reardon DA, Wen PY. Glioma in 2014: unravelling tumour heterogeneity-implications for therapy. *Nat Rev Clin Oncol*. 2015;12(2):69–70.
44. Ozawa T, Holland EC. Rethinking glioma treatment strategy. *Oncotarget*. 2014;5(20):9532–9533.